2023

Investigating Neuroanatomical Evolution through Proliferative Cells in the Astyanax Mexicanus

Sophie Staeger

Investigating Neuroanatomical Evolution through Proliferative Cells in the *Astyanax Mexicanus*

A Thesis Presented

by

Sophie Staeger

To the Keck Science Department

Of Claremont McKenna, Pitzer, and Scripps College

In partial fulfilment of

The degree of Bachelor of Science.

Senior Thesis in Neuroscience

December 12, 2022

Table of Contents

Abstract

The *Astyanax mexicanus* is a single species of fish that has two very distinct morphs, the cave fish and the surface fish. 200,000 years ago, cave fish ancestors entered the dark and challenging cave environment of Mexico and were forced to adapt in order to survive. Such adaptions include larger fat reserves, more sensitive olfaction, increased neuromasts, and a unique nervous system structure. Yet, other functions regressed, as they lost their eyes and pigmentation. The Duboué lab has established a clear reciprocal relationship between the volume of structures involved in the neuronal adaptations, but the biological mechanisms underlying the development of these traits are still unknown. Altered distribution of proliferative, or replicating, cells early in development might be contributing to the unique neuroanatomy of each morph. We predicted that proliferating cells destined for the optic tectum in surface fish are instead redirected to the hypothalamus in cave fish. By modifying a technique typically used for isolated cell culture, called EdU (5-Ethynyl-2'-deoxyuridine) immunostaining, we aimed to detect proliferative cells in the *Astyanax* model system. In the embryonic stage of development, EdU was incorporated into the DNA of proliferative cells, then at 6 days post fertilization, cells expressing EdU in their DNA were stained with Alexa fluor dye to reveal their location. The protocol was successful, and preliminary data showed increased optic proliferation in surface fish, supporting the hypothesis. Observing the translocation of proliferative cells in cave fish and surface fish has allowed for clarification into the mechanisms of neuroanatomic evolution that can in turn be used to inform general models of how animal brains evolve to ever changing external conditions.

Introduction

Evolution of the Vertebrate Brain

Evolution of the vertebrate brain is apparent in the divergent morphology and behavior seen across the animal kingdom, yet our understanding of the general principles that underly its evolution remains poorly understood. The majority of vertebrate brains, from fish to human, share the same division of structures, including the olfactory bulb, cerebellum, cerebral hemispheres, medulla oblongata, olfactory bulb, optic tectum, and pituitary gland. Although, overall brain size varies across vertebrate species, along with the proportionality of each region. It is widely accepted that neuroanatomical variation across vertebrate species is a result of many ontogenetic mutations that determine the developmental trajectory of a species (Northcutt, 2002).

It is crucial to understand the origin of the characteristic vertebrate brain in order to address how humans could be evolving today. Vertebrate brains all contain similar regions and proximal orientation, with the only known exceptions in the lamprey and hagfish, that lack a cerebellum. The preservation of these major organizational trends across nearly all vertebrate species indicates that this organization of the nervous system arose concordantly with the appearance of vertebrates or soon after. *Haikouella*, a chordate from the Lower Cambrian period, is among the earliest representations of the established vertebrate nervous system. Its brain is estimated to have "two or three rostro-caudal lobes" and evidence of "laterally paired eyes," that suggest the chordate possessed a diencephalon or midbrain. Some hypothesize that the most rostral region of the brain was bilobular, indicating the presence of cerebral hemispheres. Yet, many comparative biologists doubt the theory due to the lack of an olfactory center, which is thought to be the origin of the cerebral hemispheres (Northcutt, 2002). Another discovery made in 1999, found a fossil of a low Cambrian chordate called *Haikouichthys* that presented a head with a skull, as

seen in craniates today, which indicated that cerebral divisions of the vertebrate nervous system were present initially in a species of chordates showing craniate anatomy (Northcutt, 2002).

It is evident that vertebrates have evolved tremendously in the past 500 million years since the Cambrian explosion, whether it be in overall size or connectivity **(Figure 1)**. And even though vertebrate nervous systems maintain basic structural similarities, there is a high degree of size difference across vertebrate species. There is a 30-fold difference in brain size (relative to body mass) over all vertebrate radiations, a distinction referring to a grouping of vertebrates that descended from a single parent species, and quickly adapted, increasing species biodiversity. For instance, agnathans; the brains of hagfishes are two to three times bigger than those of lampreys
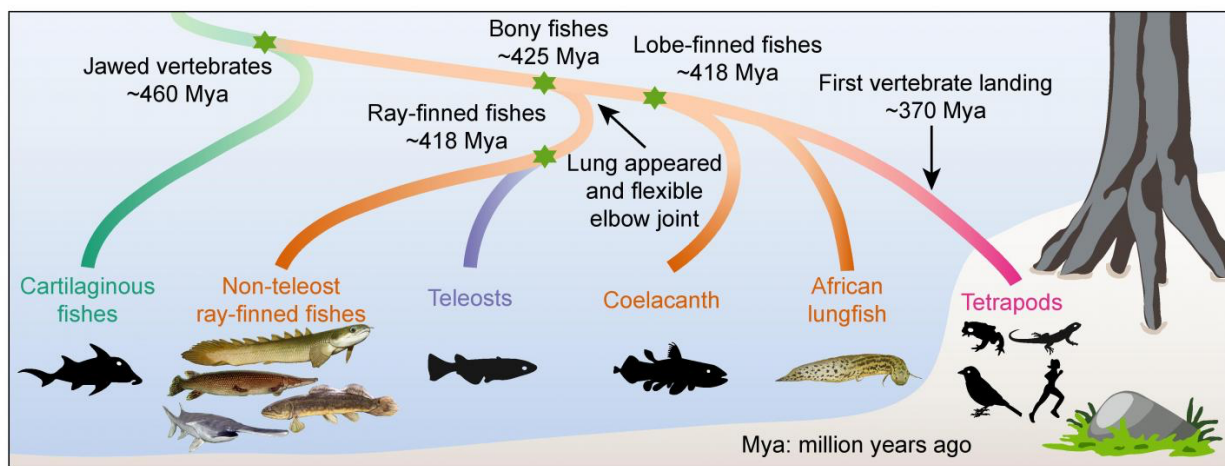
Figure 1: A general overview of vertebrate evolution over time (Zhang, University of Copenhagen, n.d.).

with the same size body. Also, bony fishes possess comparatively larger brains than agnathans do, with teleosts, such as the *Astyanax mexicanus*, showing larger volume than non-neopterygians (bichirs, paddlefish, sturgeons). Teleosts, also called ray-finned fishes, have comparably smaller brains than most amphibians and reptiles, and reptilian brains are approximately 2-3 times the size of amphibian brains. Mammalian and avian brains range between 6-10 times the size of reptilian brains relative to body mass, with mammals being 10 times larger on average. The largest brain sizes relative to their body, are primates and cetaceans.

Currently, bony fishes, amphibians, and reptiles exhibit considerable overlap in relative brain size as a result of distinct environmental pressures that selected for volumetric increases or decreases in neural tissue.

When the center of the nervous system increases in size, it also leads to a surge of neural centers with more diversity of neural cells within each; as a result, the vertebrates exhibit more behavioral intracity. Neural centers, synonymous to nuclei, are a "complex couplings or association stations between two orders of elements: the sensory conductors, that bring the neural excitation, and the motor conductors, that propagate the latter to the corresponding locomotor and glandular apparatuses" (Ramon y Cajal, 1999, p. 249). The modifications of the optic tectum demonstrate the clear effect of size on function; the optic tectum is a brain region associated with visual perception, and in all species with a skull, it is comprised of cellular and fibrous layers called laminae. The neural evolution of amniotes (reptiles, birds, and mammals) from hagfishes was associated with increased laminae in the tectum, in which cellular layers would perceive additional sensory stimuli and connect to unique neural centers. The relative size of the optic tectum and the quantity of laminae within the region is associated with more developed vision. Ray-finned fishes also exhibit increased tectal lamination, following the progression from lypteriformes to teleosts, as seen in the *A. mexicanus*, the model organism referenced later in this paper, which maintains the same positive trend between laminae and vision development.

Evolution of the telencephalon in craniates, specifically their cerebral hemispheres, also shows increased abundance of neural centers following forebrain enlargement. Ray-finned fishes

gain neural centers most evidently in their pallium (Northcutt, 2002). As the cerebral

hemispheres exhibit more lamination and increases in neural centers, subdivisions arise, that are

similar to those of the mammalian cerebral cortex, although on a smaller scale. To evaluate the

relative enlargement of neural centers on its present cell classes, the cerebral cortex, cerebellum,
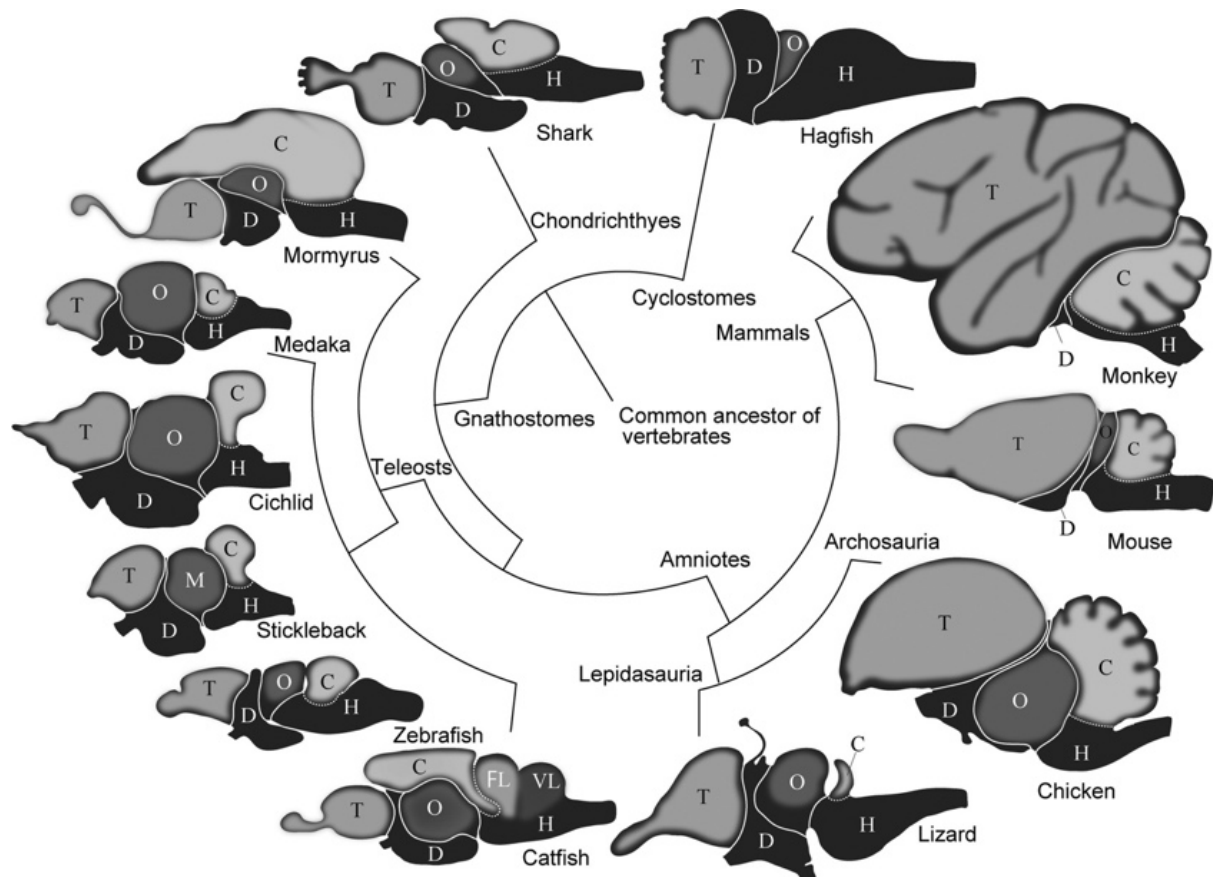
Figure 2: The evolution of the vertebrate brain, highlighting variation in size and proportionality of the cerebellum (C), diencephalon (D), facial lobe (FL), hindbrain (H), optic tectum (O), telencephalon (T), and vagal lobe (VL), with the earliest being the hagfish brain and the most recent being that of the monkey. (Kawakami, 2017, p. 160).

olfactory bulb, and optic tectum are often observed (**Figure 2**). Between anamniotes (fishes and

amphibians) and amniotes (reptiles, birds, mammals), cerebral and olfactory centers are

unchanged in the amount of present cell classes, although the optic tectum exhibits more

diversification of cell classes as brain size rises. It is clear that there are similarities in all

vertebrate brains, but what differs most are their relative sizes and associated increases in lamination, quantity of neural centers, and function.

Brain size is relevant because brains are ultimately centers for processing environmental stimuli that facilitate the survival of a species by eliciting the advantageous physiological responses to a given situation, whether it be through cognition, instinct, or reflex. Northcutt states "as brains increase in size, the number of the neurons and their interconnections also increase, thus expanding the available equipment for processing information" (Northcutt, 2002, p.750). Higher capacity for processing heightens one's perception of the physical world, resulting in more complex motor outputs and better performance on novel behaviors that enhance survival.

Neuroanatomical Adaptions in Ray-Finned Fishes

To comprehend how the human brain is adapting to today's environment, the mechanisms of evolution that have led to the development of our species must be understood. Trait distinction appears to be derived from ontogenetic change, affecting a developmental stage the nervous system, and also the selection of traits dependent on the environment. For example, the lateral line present in all fish arose because protein terminal truncation generated a shorter protein that encodes for placodal development. Also, similar driving forces are behind ray-finned fishes' unique cerebral hemisphere development. The trend can be dated back to differences between Devonian ray-finned fishes and Devonian sharks. They differ in size, with sharks being much larger at 1-2m while the fishes were less than 15cm according to fossil evidence. The associated size difference in larvae implies the small nature of ray-finned fish's prey, indicating the need for visual acuity, that advanced the development of optic brain regions. In the majority

of vertebrates, the forebrain vesicle becomes a hollow tube with a "germinal layer that can be divided into ventrodorsal series of ones lying adjacent to the central lumen or prosencoel" (Northcutt, 2002, p. 752-753). Northcutt states that "the lateral walls of the rostral half of the forebrain vesicle expand more rapidly than do the floor or roof and bulge out to form cerebral hemispheres," resulting in the "inversion of the initial, most dorsal segment of the dorsal half (pallium) of the forebrain vesicle" (Northcutt, 2002, p. 753). Contrarily, ray-finned fishes have a
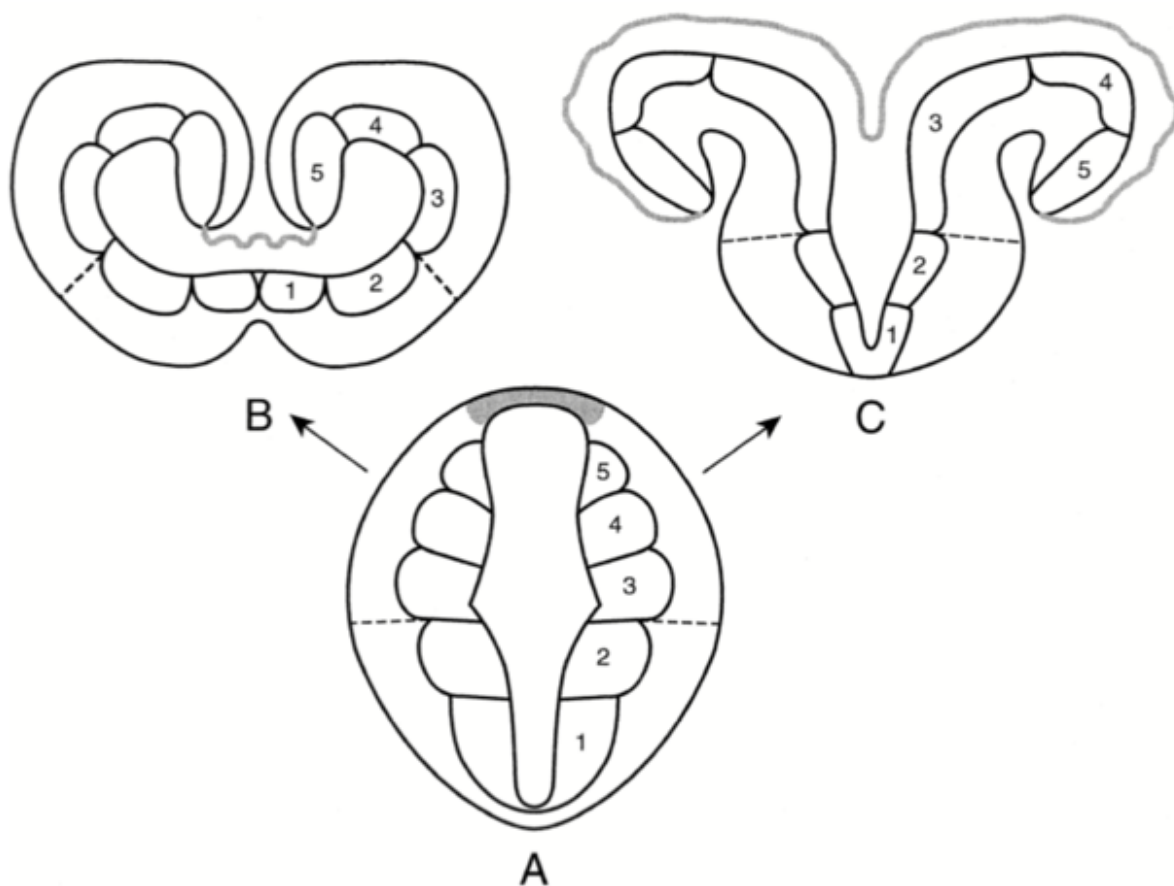

Figure 3: A "schematic representation of transverse sections through the initial forebrain vesicle (A), the evaginated cerebral hemisphere of an amphibian (B), and the everted cerebral hemispheres of a ray-finned fish (C). The topography of the germinal zones (1–5) of their germinal zones (1-5) and their derivatives are profoundly altered by th process of evagination versus eversion, as is the extent of the choroid plexus (gray). Both types of cerebral hemispheres can be divided (dashed line) into a ventral subpallium (1,2) and dorsal pallium (3-5). While the topographical relationships of the cell groups of the subpallium are hardly changed, the topography of the pallial cell groups of ray-finned fishes is revered lateromedially when compared to the pallial cell groups of an amphibian. Modified from Northcutt (1995)" (Northcutt, 2002, p. 753).

pallium that becomes thick and everts, causing the most dorsal segment of the pallium to reside

alongside the pallium (**Figure 3**). The change in neural development might have occurred

because in such small organisms with little intracranial space, gaining better eyesight would be

associated expansion of the optic tectum, making evaginated cerebral hemispheres implausible,

and instead forcing an everted formation to compensate for increasing size of eyes and optic

regions. Everted development of cerebral hemispheres in the telencephalon was not selected for

directly but instead was a repercussion of ray-finned fishes' reduced body size and selection for

visual acuity in their larvae (Northcutt, 2002).

Astyanax Mexicanus Model System

Observing the *Astyanax mexicanus,* a freshwater teleost fish*,* will allow for an enhanced

understanding of trait evolution in the brain, and more specifically, how neuroanatomical

changes can lead to evolutionarily adaptive behaviors. Native to the rivers of Texas and Mexico,

the *Astyanax mexicanus* is a single species with two distinct morphologies, one that inhabits the

surface, (**surface** fish) and one that inhabits cave systems (**cave** fish; **Figure 4**). Cave fish were

discovered in the Sierra de El Abra in Tamaulipas and San Luis Potosí, Mexico (Jeffery, 2020;

Figure 5). Named after their native cave, the Pachón was the model organism of the Duboué

laboratory at Florida Atlantic University. The two morphs diverged about 200,000 years ago

when the ancestral surface-dwelling *Astyanax* became trapped in the intricate cave systems of
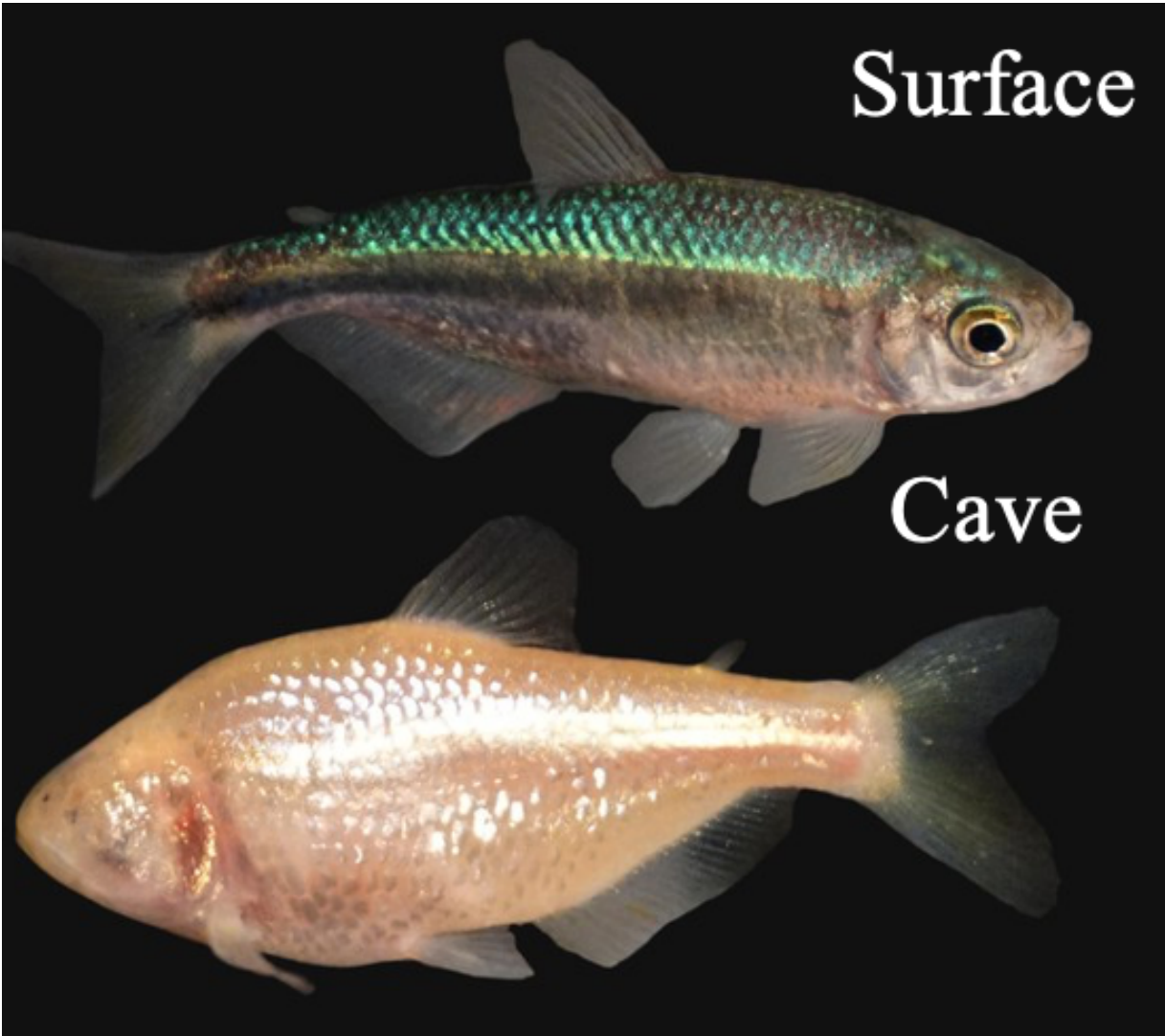
Figure 4: Portrayal of the clear phenotypic differences between the A. Mexicanus surface morph (top) and cave morph (bottom).

Mexico due to a rise in water levels during the rainy season. Adults are 8-10mm long, and as an r-selected species, release hundreds of eggs during spawning. Following fertilization, offspring develop very quickly with gastrulation starting at 6 hours post fertilization (hpf) then hatching from chorion at 1 day post fertilization (dpf). It takes approximately 6-8 months for offspring to become sexually mature, and they typically live for about 10 years.
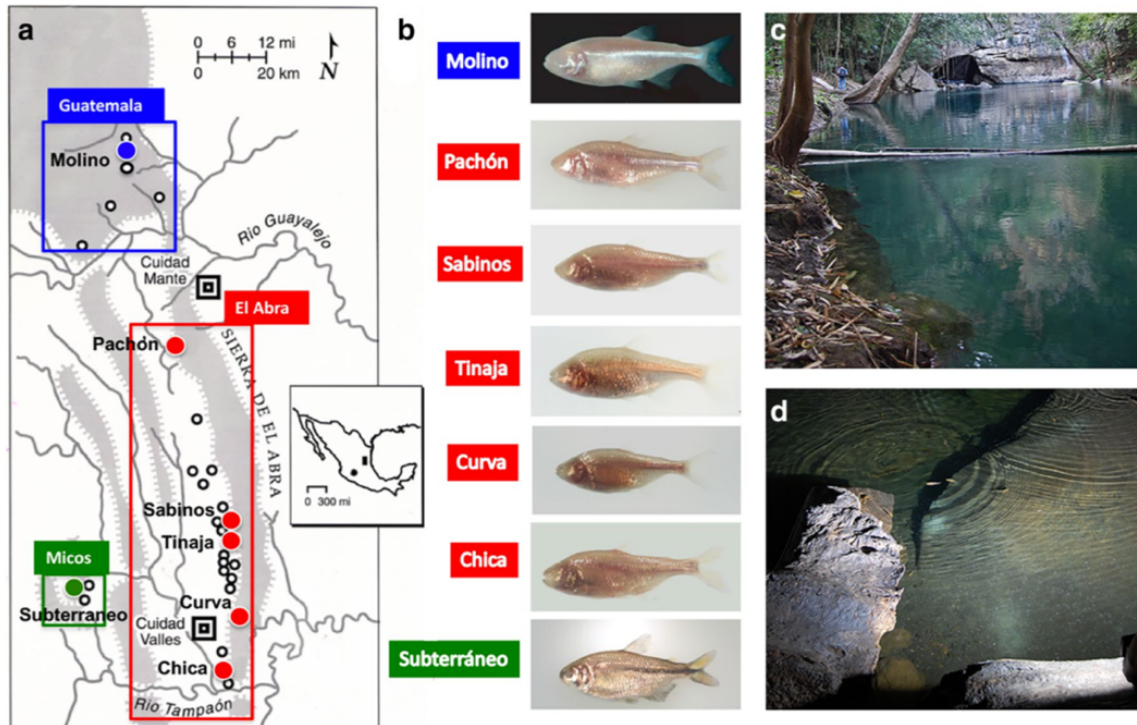
Figure 5:"Astyanax caves, cave fish populations, and habitats. **a**. A map showing the distribution of caves in the El Abra region of Tamaulipas and San Luis Potosí, Mexico. Boxes outlined in blue, red, and green show locations of Astyanax caves in the Sierra de Guatemala, Sierra de El Abra, and Micos regions, respectively. Mexico map showing the locations of A. Mexicanus cave fish in the Abra epicenter (right shaded rectangle) and A. aeneus cave fish in Guerrero (left shaded sphere). **b**. Most frequently studies cave fish populations in the Guatemala (blue label), El Abra (red labels), and Micos (green label) regions. **c**. A surface fish habitat at El Nacimiento del Río Choy. **d**. A cave fish habitat in El Sótano de Las Piedras." (Jeffery, 2020, p.2).

The two morphs are phenotypically distinct, with cave fish lacking both eyes and pigment, as well as neuroanatomically unique. Eyes are completely absent in the cave fish, as they lost usefulness within a completely dark environment. Forced to survive in an isolated setting, cave fish evolved traits advantageous to their new surroundings. They present more taste buds, more teeth, neuromasts, and larger fat reserves (associated with slower metabolism). They also developed vibration attraction behavior, that can identify external frequencies of less than 50Hz,

likely made possible by their abundance of neuromasts along their lateral line. Such neuromasts develop only after the disappearance of the eyes, at approximately two months of age, indicating that this is a connected process (Rétaux et al, 2015).
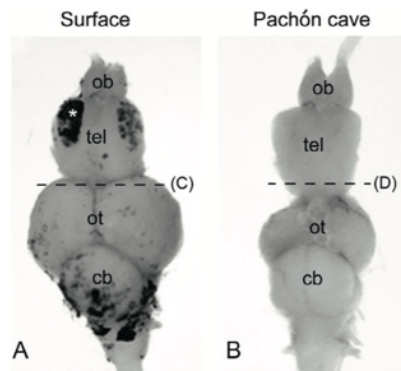
Figure 6: "Adult brains in *Astyanax* surface fish and Pachón cave fish. A and B show dorsal views of adult brains after dissection (anterior is up). The two individuals were of identical size (4 cm standard length). The dotted lines indicate the approximate section levels shown in C and D. Ob, olfactory bulbs; tel, telencephalon; ot, optic tectum; cb, cerebellum. C and D show frontal sections through the head of the adult fish, after Kluver and Barrera coloration. The arrowheads on the Pachón picture show degenerated and cystic eye, partially calcified (dark/purple) and covered by skin. R, retina; l, lens; on, optic nerve; ot, optic tectum; s, skin" (Rétaux, 2016, p. 229).

The cave fish brain is slimmer and more elongated than the surface fish brain due to a clear decrease in tectal volume in the midbrain or mesencephalon (**Figure 6**). The optic tectum shows a 50% decrease in volume and 20% fewer neurons comparative to the surface fish. Although, the telencephalon is expanded, including the olfactory bulbs, pallium, and subpallium. The diencephalon shows fewer in optic nerve fibers yet a total increase in volume within the hypothalamus and thalamus (Rétaux, 2011). The metencephalon, or hind brain, is structurally similar and constant in volume across the morphs. Interestingly, cave fish embryos develop the rudiments of eyes, specifically the optic cup and abnormally small lens, but all retinal cells systematically degenerate following apoptosis of the lens (Jeffery, 2020). Indeed, studies suggest that the frontal regions of the brain could not develop without simultaneous cellular processes associated with initial eye formation (Rétaux et al, 2011).

The advancement of their olfactory lobes and sensory organs allows for an enhanced ability to find food without light, and slower metabolism increases fat storage, specifically in the oversized liver, allowing the morph to better maintain their weight during times when resources are scarce. They also display intense appetites even during periods of high nutrient availability that is associated with a mutated *mcr4r* gene, involved in the production of the amino acid, leptin. Overeating often results in very high levels of blood sugar, but their insulin receptor is mutated, allowing cave fish to be resistant to excessive absorption of glucose in somatic cells, although, other traits regressed as previously mentioned, such as pigmentation (melanin), eyes (vision), schooling behavior, aggression, and circadian rhythms. Morphs also differ in their feeding behavior, locomotion, structure of craniofacial bones (Jeffery, 2020).

Shh is a morphogen that is highly expressed in cave fish embryos near the anterior midline that plays a role in mediating vision loss. Shh is a developmental signaling molecule that mediates taste bud development and increased jaw size in cave fish. The role of the morphogen was verified with the artificial overexpression of Shh in surface fish that resulted in eye reduction, a more pronounced jaw, and more taste buds.

Ventral Expansion and Dorsal Contraction in Cave Fish

Hypothalamic expansion involves the redistribution of ventral retinal cells (Jeffery, 2020). The mechanism is not well understood but Pottin et al hypothesized that the medial cells of neural plate that are destined for the ventral retina instead become the hypothalamus (Rétaux, 2011) (**Figure 7**). There is a larger the hypothalamus of cave fish morph associated with more

proliferation than the surface fish. The proliferation is localized in the hypothalamus and preoptic

region, more ventrally, but it is not exhibited

dorsally in the diencephalon or mesencephalon.

Proliferation appears to be dependent on the *Shh*

signaling molecule because its inhibition by

cyclopamine induces a decrease in proliferation

and overall size of the hypothalamus.

Neurogenesis could also be mediated by

serotonin, as cave fish express serotonin earlier

than surface fish embryos, 18hpf and 22 hpf

respectively (Rétaux, 2011). The anterior

hypothalamus has a higher concentration of

Figure 7: Comparison of the surface fish and cave fish brain in 2-photon microscope images. Blue sections highlight the optic tectum (OT) and purple sections highlight the hypothalamus (Hyp). Adapted from images seen in Kozol et al, 2022.

serotonin-expressing neurons. These neuroanatomical trends can be evaluated in a hybrid

population to investigate their genetic basis using correlations.

By analyzing an F2 hybrid generation, Kozol et al. (2022) constructed a brain atlas for cave

fish, surface fish, and hybrids to observe volumetric and geometric differentiation within
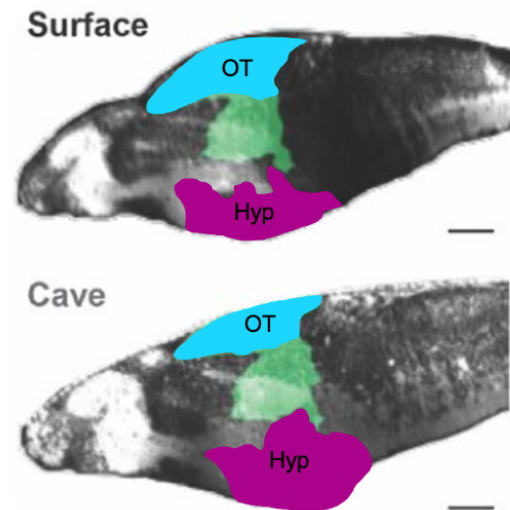
subnuclei. They found that the dorsal diencephalon, specifically the dorsal thalamus, was smaller

in cave fish, and that the intermediate and caudal hypothalamus were enlarged. To evaluate the

degree to which the evolution of structures covary, Kozol et al ran a pairwise analysis that

identified three distinct clusters showing positive correlation to the subnuclei within each.

Ventral structures were correlated in Cluster 1 and subnuclei were identified as the subpallium,

hypothalamus, posterior tuberculum, tegmentum and prepontine. Cluster 2 included dorsal and

caudal structures such as the optic tectum, cerebellum, pons, reticulopontine, and medulla

oblongata. Cluster 3 contained telencephalic structures including the subpallium and also the dorsal diencephalon (**Figure 8**).

In an F2 hybrid generation of surface and cave fish, the Duboué laboratory at Florida Atlantic University identified a negative correlation between the volume of dorsal structures, and that of ventral structures, meaning that as cluster 1 structures expand, dorsal structures would regress, and vice versa (**Figure 8**). The trend is confirmed given that the cave morph evolved a contracted optic tectum, located dorsally, along with an expanded hypothalamus, located ventrally, indicating that ventral expansion occurs at the expense of dorsal contraction. Although, the biological mechanisms underlying the development of these traits are unknown.
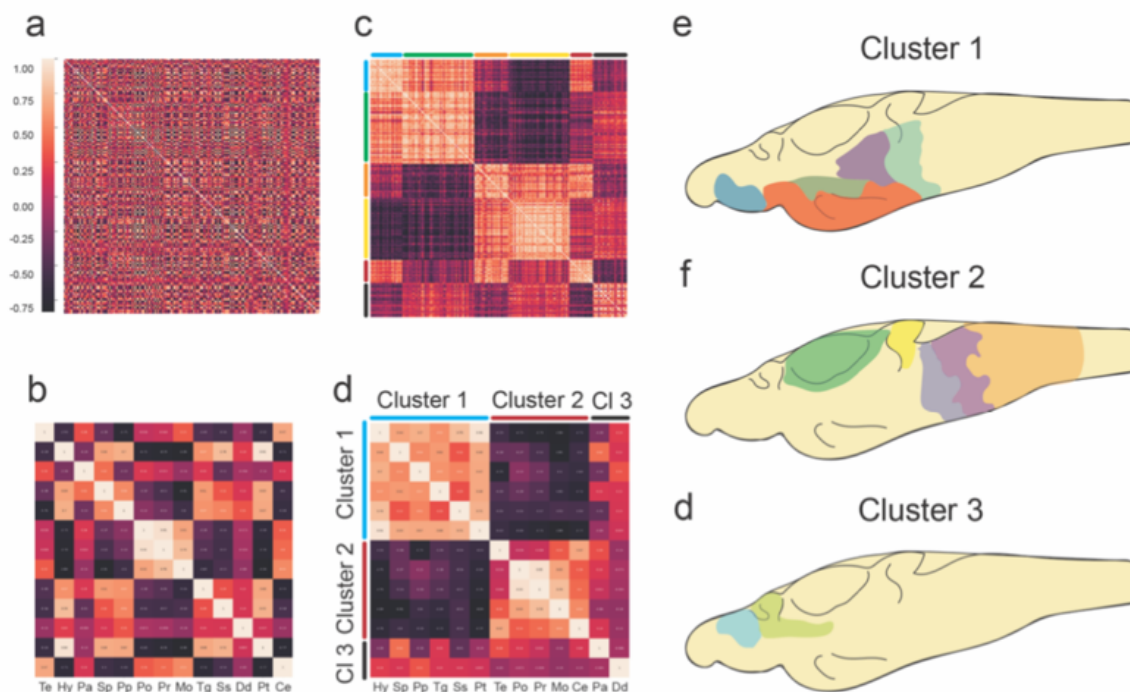
Figure 8: "Covariation of brain region size reveals developmental tradeoff between relationships dorsal-ventral clusters brain-wide. Pairwise correlation matrix comparing covariation between (**a**) all 180 brain segments and (**b**) 13 developmentally defined regions. Clustering of pairwise correlation matrices produced **c** 6 clusters of brain segments and **d** 3 clusters of brain regions that share covariation relationships. (**c**) is the clustered matrix from (**a**), while (**d**) is the clustered matrix from (**b**). Illustrations depicting clustered segments: (**e**) cluster 1 includes the subpallium (blue), hypothalamus (orange), posterior tuberculum (olive green), tegmentum (orchid purple) and prepontine (light blue) (**f**) cluster 2 includes the optic tectum (green), cerebellum (yellow), pons (light purple), reticulopontine (orchid purple) and medulla oblongata (light orange) (**g**) cluster 3 includes subpallium (sky blue) and dorsal diencephalon (yellow green)" (Kozol, 2022, n.p.).

To investigate how structural differences arise between the cave fish and surface fish, we generated a new immunostaining protocol to detect replicating cells in the embryonic stage of development. The goal was to incorporate EdU (5-Ethynyl-2'-deoxyuridine) into the DNA of proliferating cells, and once larvae matured, 2-photon imaging would reveal the location of the stained cells. We predicted that the cave fish morph would show a reduction of stained cells in the optic tectum but an increase in the hypothalamus due to proliferative cells being redirected from dorsal regions to ventral regions. Given the genetic and neuronal similarities between fish and high order mammals, the findings would elucidate mechanisms of evolution that can in turn be used to inform predictive models of how the human brain adapts to an ever-changing society.

Methods

The objective of the experiment was to develop a protocol to investigate how neuroanatomical changes arise between *Astyanax mexicanus* morphs, the cave fish and the surface fish. In order to observe the mechanisms of divergent evolution in the *Astyanax* nervous system, the protocol would breed both morphologies separately and incorporate 5-Ethynyl-2'-deoxyuridine (EdU) into the DNA of proliferative (replicating) cells during the embryonic stage of development. Then as the larvae matured, cells expressing EdU in their DNA would be stained with Alexa fluor 555 dye using Click chemistry that reacts the azide present in the dye with the alkyne in the EdU. Then, EdU positive cells would be regionalized using t-ERK (total extracellular-regulated kinases) antibodies that stain and outline the entire brain. Perfection of this protocol would allow for 2-photon microscopy revealing the anatomical location of cells proliferative at the embryonic stage. Later quantification of proliferative cells in certain brain regions, specifically optic tectum and hypothalamus, could identify differences and demonstrate altered translocation of proliferative cells early in development across *Astyanax* morphologies. Duboué and Kozol's hypothesis is that the cave fish morph would show a relative reduction of stained cells in the optic tectum with an increase in the hypothalamus assuming proliferative cells are redirected from dorsal regions to ventral regions.

Table 1. Solutions in Click-iT EdU Kit (Thermo Fisher Scientific, n.d., n.p.)

Material	Expires	Storage*
EdU **(1)**	1 year	-20C, avoid light
Alexa Fluor azide 555 nm **(2)**	1 year	-20C
DMSO **(3)**	-	4C

Click-iT EdU reaction buffer **(4)**	6 months	4C
CuSO4 **(5)**	-	4C
Click-iT EdU buffer additive **(6)**	1 year (If solution develops a brown color, it is degraded and should be discarded)	-20C
Hoechst 33342 **(7)**	-	4C

Preparing Stock Solutions

In order to prepare the stock solutions from the Click-iT EdU Kit, vials were warmed to room temperature before opening (**Table 1**). First, a 10mM stock solution of EdU, component A, was prepared by mixing the total volume of EdU (1) with 2mL of DMSO (3). Next, a working solution of Alexa Fluor azide (555nm), component B, was prepared by adding the entire volume of Alexa Fluor azide (2) to 70uL of DMSO (3). The working solution of 1X Click-iT EdU reaction buffer, component D, was made by transferring all reaction buffer solution (4mL) in the **(4)** bottle into 36mL of dH$_2$O. The bottle (4) was rinsed with some of the diluted solution to ensure the transfer of all of the concentrate. Finally, the 10x stock solution of Click-iT EdU buffer additive, component F, was made by adding 2mL dH$_2$O to all the Click-iT EdU buffer additive (6) and was mixed until fully dissolved.

Table 2. Stock and Working Solutions (Thermo Fisher Scientific, n.d., n.p.)

| Solutions	Concentration	Label
(Stock) EdU in 100% DMSO	**10mM**	**A**
(Working) Alexa Fluor azide 555 nm with DMSO	**N/A**	**B**
(Working) Click-iT EdU reaction buffer	**1X**	**D**
(Stock) Click-iT EdU buffer additive	**10X**	**F**

Trial 1

Husbandry

The first trial of the protocol was performed with zebrafish, or *danio rerio*, due to the convenience of their breeding, which requires less preparatory time than the *Astyanax.* Three crosses were set up the night before egg collection to allow for proper acclimation. Each tank contained a divider separating males and females, that was lifted in the morning. Crosses were set up in a 2:1 female : male ratio, as lab technicians found that ratio most effective in the past. At 8:00am , the dividers were removed and the water was replaced with fresh system water. The tanks were monitored closely and checked every 15 minutes. When eggs were present, they were collected, labeled with the time of the drop, and aged using Figure 9. The viable embryos were sorted and raised until 10 hours post fertilization (hpf). A developmental staging table was used for reference (**Figure 10L**).
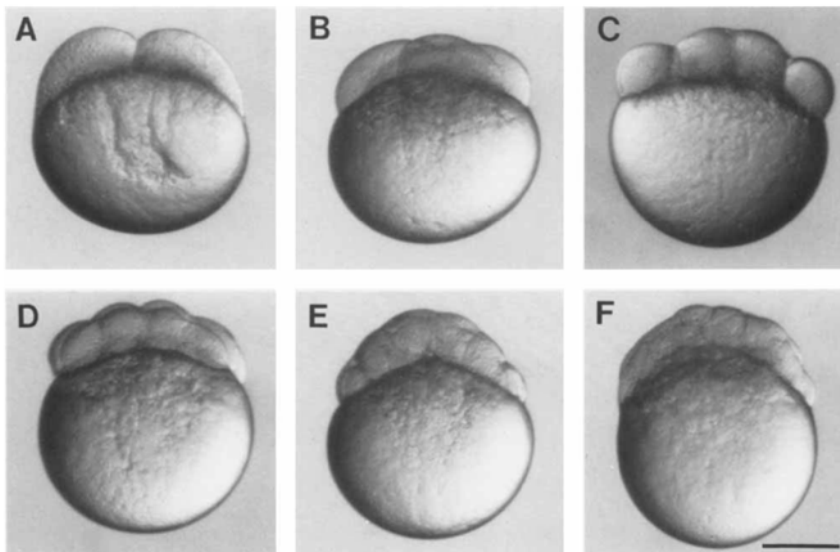
Figure 9: Images show the development of zebrafish embryos from 0.75 hours post fertilization (hpf). A depicts the two-cell stage at 0.75 hpf. B shows the four-cell stage at 1 hpf. C is the eight-cell stage at 1.25 hpf. D is the sixteen-cell stage at 1.5 hpf. E is the thirty-two-cell stage at 1.75 hpf. F shows the sixty-four-cell stage at 2 hpf. (Kimmel, 1995, p. 262).
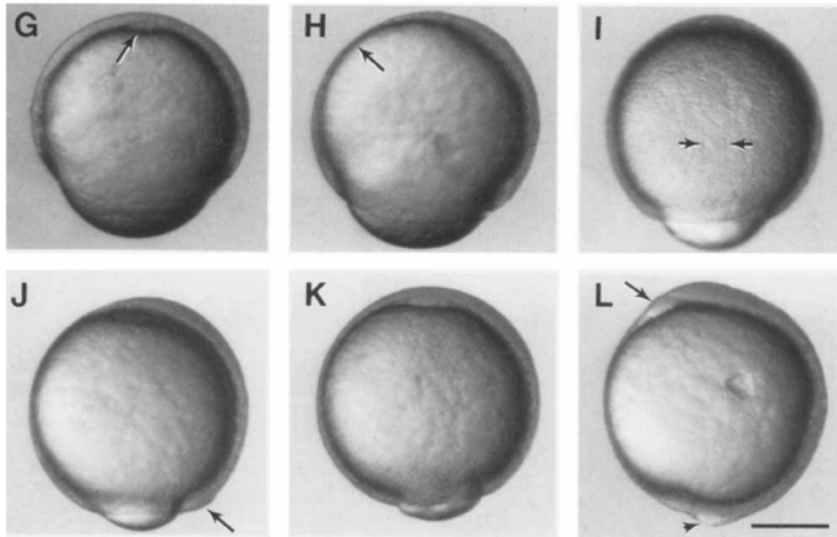
Figure 10: The developmental staging table shows appearance of embryo between 7.7 hpf and 10hpf. G: 7.7 hpf. H: 8 hpf. I: 8.4 hpf. J: 9 hpf. K: approximately 9.5 hpf. L: bud stage at 10hpf. (Kimmel, 1995, p. 269).

EdU Incubation

Eight embryos were placed in 1mL of 500uM EdU/10% DMSO system water in 1.5mL microcentrifuge tube. The proper concentration was acquired by pipetting 50uL of 10mM EdU in 100% DMSO (stock solution A) into 950uL of system water. The process was repeated for two microcentrifuge tubes. Each tube was incubated on ice for one hour, then larvae were transferred back into system water and kept at 23°C. Larvae were sacrificed at six days post fertilization (dpf) and fixed for 4.5 hours in 4% paraformaldehyde (PFA) at room temperature. Following fixation, three 5-minute washes were performed with 1xPBSTx(0.25%) rocking at 4°C.

Staining EdU

Samples were permeabilized for one hour in 1xPBS / 1% DMSO / 1% Tritonx100 at room temperature. Each tube received 790uL dH$_2$O, 100uL 10xPBS, 100uL 10% Triton, and 10uL 100% DMSO to achieve the desired concentrations. The 1X Click-iT EdU buffer additive was prepared by diluting 10uL of 10x buffer additive with 90uL of dH$_2$O. In order to make the

Click-iT reaction cocktail, which would stain the EdU molecules, the following volumes were added in order 860uL 1x reaction buffer, 40uL $CuSO_4$, 2.5uL Alexa Fluor, and 100uL of the buffer additive made in the previous step. The permeabilization solution was replaced with the reaction cocktail immediately and protected from light. Samples were incubated for one hour at room temperature rocking. Following the stain, samples were washed five times (5 minutes each) with 1xPBSTx(0.25%) to remove the cocktail. 2-Photon microscopy revealed that the stain was unsuccessful so the protocol was modified to increase penetration of EdU and absorbance of the Alexa Fluor.

Trial 2

Husbandry

For the second rendition of the protocol, cave fish were bred, specifically the Pachón, named after the cave system from which it originates. Three tanks received heaters one day prior to predicted spawning. Heaters were set to 84 degrees Fahrenheit because a slow increase of temperature from 72°F – 78°F is optimal for maximizing eggs drops and quality of embryos (Ma, 2021). Embryos were collected at 7:30am, then aged and sorted
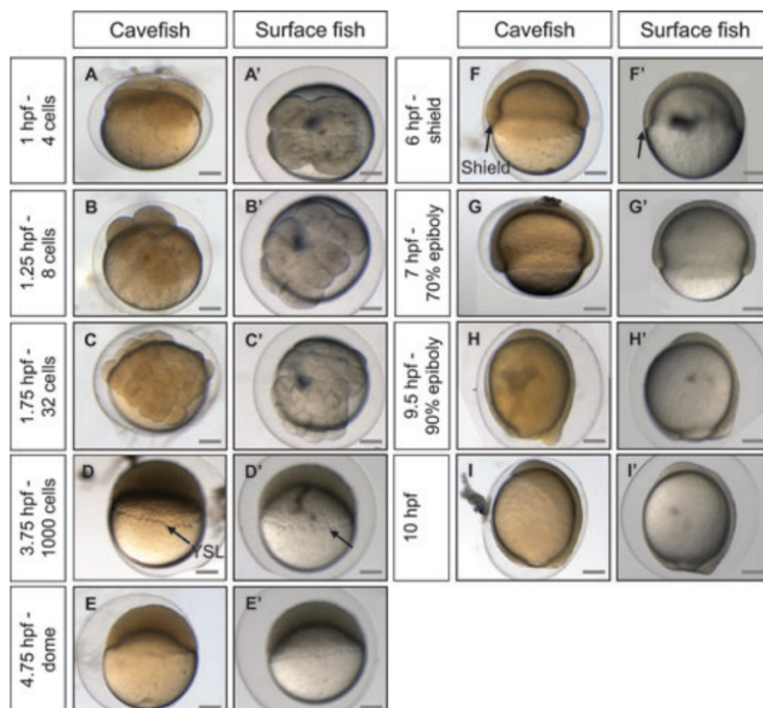
Figure 11: Images compare cave fish and surface fish larvae from 1 hour post fertilization to 10 hours post fertilization. (Hinaux, 2011, p. 156).

immediately after being transferred into system water. Developmental staging tables in Figure 11 was used for initial aging of embryos.

Modifications to Protocol

To elicit better penetrance of the EdU, the protocol increased the concentration of DMSO for EdU incubation to concentration to 15% instead of 10%. The proper concentration was acquired by pipetting 900uL of system water, 50uL of 10mM EdU in 100% DMSO (stock solution A), and 50uL of 100% DMSO. EdU staining procedure remained consistent between the first and second trial. In addition, acetone incubation was added to ensure penetrance of the Alexa Fluor azide. Following permeabilization, samples were quick-washed with deionized water (dH$_2$O), then placed in acetone at -20°C for seven minutes. Quick wash was repeated. Alexa-Fluor staining proceeded performed in the first trial.

Immunohistochemistry was then incorporated to map the entire brain of the larvae and identify the location of Alexa-stained cells. First, samples were blocked in 1% sheep serum / 1% bovine serum albumin (BSA) / 1x PBSTx (1%) at room temperature for 1.5 hours. The volumetric measurements per test tube were as follows: 750uL dH$_2$O, 100uL 10% BSA, 100uL 10xPBS, 25uL TritonX100, 20uL sheep serum, 10uL 100% DMSO. After blocking, the samples were incubated in the primary antibody for three days rocking at 4°C. The primary antibody solution used was 1% BSA / 1% DMSO / 1xPBSTx(1%)/1:500 antibody); the volumetric measurements per test tube were as follows: 761uL dH$_2$O, 100uL BSA, 100uL 10xPBS, 25uL 100% DMSO, 2uL tERK: p44/42 MAPK(Erk1/2)(L34F12) Mouse mAb #4696. On the morning of the third incubation day, the samples underwent three 20-min washes with 1xPBSTx(0.25%) rocking at 4°C. The wash was replaced with secondary antibody solution that was 1% BSA/ 1% DMSO / 1xPBSTx(0.25%) / 1:1000 antibody). Each tube received 763 uL dH$_2$O, 100uL 10%

BSA, 100uL 10xPBS, 25uL TritonX100, 10uL 100% DMSO, 1uL anti-mouse 488 IgGI. Left

overnight rocking at 4°C. Secondary antibody was washed out three times for 5 min with 1XPBS

and then mounted on slides for imaging on the 2-photon microscope. Scans were taken as

Z-stacks.

Performing the protocol with the aforementioned modifications, but for a range of conditions,

as shown in Table 3, including duration of EdU incubation, developmental stage of larvae, and

length of fixation.

Table 3. Conditions for Different Sample Treatments

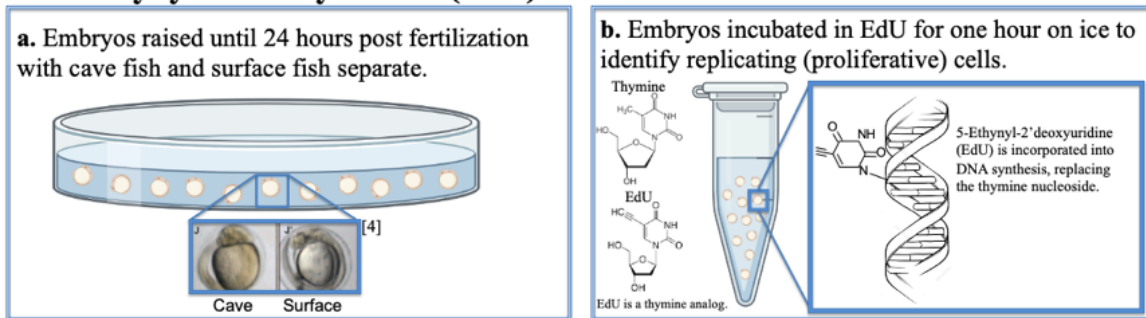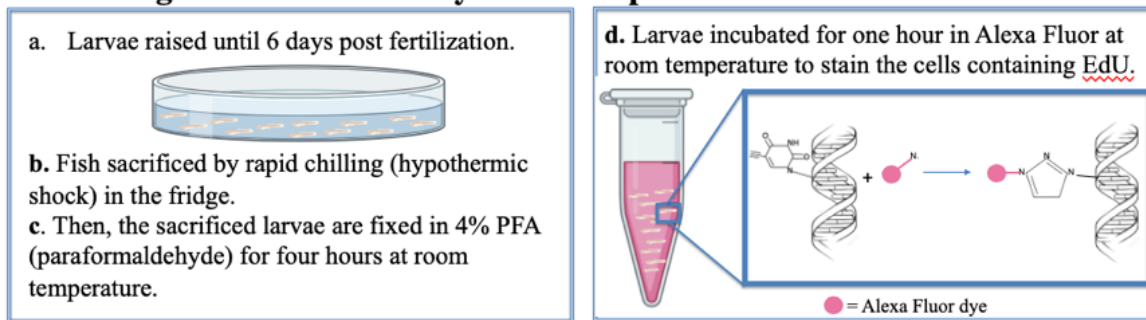| Fixation Time	A: 1 Hour at 4°C (10hpf)	B: 4 Hours at 4°C (10hpf)	C: 12 Hours at 4°C (10hpf)
I: 90 Minutes at 24 hpf	AI	BI	CI
II: 2 Hours at 3 dpf	AII	BII	CII
III: 4 Hours 6 dpf	AIII	BIII	CIII

Trial 3 (Final)

Husbandry

Day 1 began the preparations for planned cave fish (Pachón) and surface fish spawning.

They were each kept in separate tanks, with both female and male fish. Depending on the size of

the tank, the number of fish in each ranged from four to ten. Three cave fish, or Pachón, tanks

were prepped, while six were prepped for surface fish given the inconsistency in their recent egg

drops. The population of surface fish at the Duboué laboratory had proven to be more

inconsistent with breeding. Surface fish require heaters in their tanks two days prior to the

morning of an expected egg drop, while the cave fish received heaters in their tanks one day

prior. Heaters were set to 84 degrees Fahrenheit as in the second trial. Embryos were collected at

7:30am, then aged and sorted immediately after being transferred into system water. Figure 11

was used again for accurate aging of embryos.
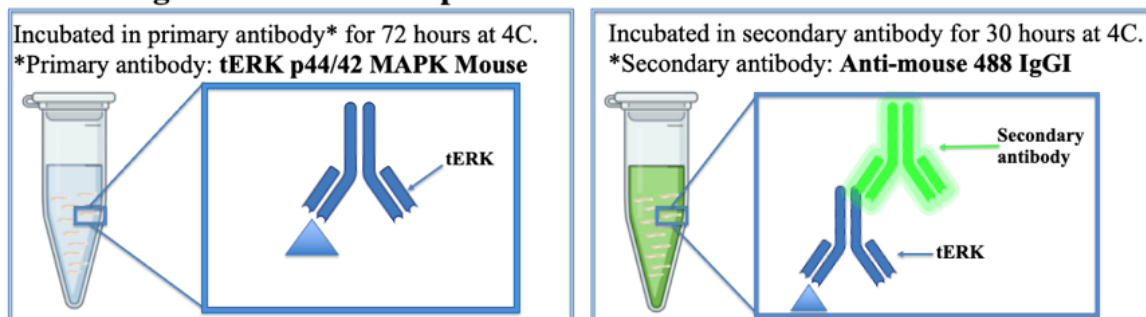
Modifications to Protocol

1. 5-Ethynyl-2'-deoxyuridine (EdU) Incubation.

a. Embryos raised until 24 hours post fertilization with cave fish and surface fish separate.

b. Embryos incubated in EdU for one hour on ice to identify replicating (proliferative) cells.

Thymine

5-Ethynyl-2'deoxyuridine (EdU) is incorporated into DNA synthesis, replacing the thymine nucleoside.

EdU

EdU is a thymine analog.

Cave   Surface   [4]

2. Staining with Alexa Fluor dye to detect proliferative cells.

a.   Larvae raised until 6 days post fertilization.

d. Larvae incubated for one hour in Alexa Fluor at room temperature to stain the cells containing EdU.

b. Fish sacrificed by rapid chilling (hypothermic shock) in the fridge.
c. Then, the sacrificed larvae are fixed in 4% PFA (paraformaldehyde) for four hours at room temperature.

● = Alexa Fluor dye

3. Staining with t-ERK to map the entire larvae brain.

Incubated in primary antibody* for 72 hours at 4C.
*Primary antibody: **tERK p44/42 MAPK Mouse**

tERK

Incubated in secondary antibody for 30 hours at 4C.
*Secondary antibody: **Anti-mouse 488 IgGI**

Secondary antibody

tERK

Figure 12: Diagrams reveal the mechanisms for each major component of the protocol, 5-Ethynyl-2'-deoxyuridine (EdU) incubation, staining with Alexa Fluor 555, and t-ERK immunohistochemistry.

The protocol for AIII conditions was repeated for both cave fish and surface fish morphologies (**Figure 12**). Larvae were raised to 24 hpf, instead of the 10hpf, to identify fewer cells and observe better differentiation. The *Astyanax* developmental staging table (**Figure 13**) was a reference for 24hpf larvae.
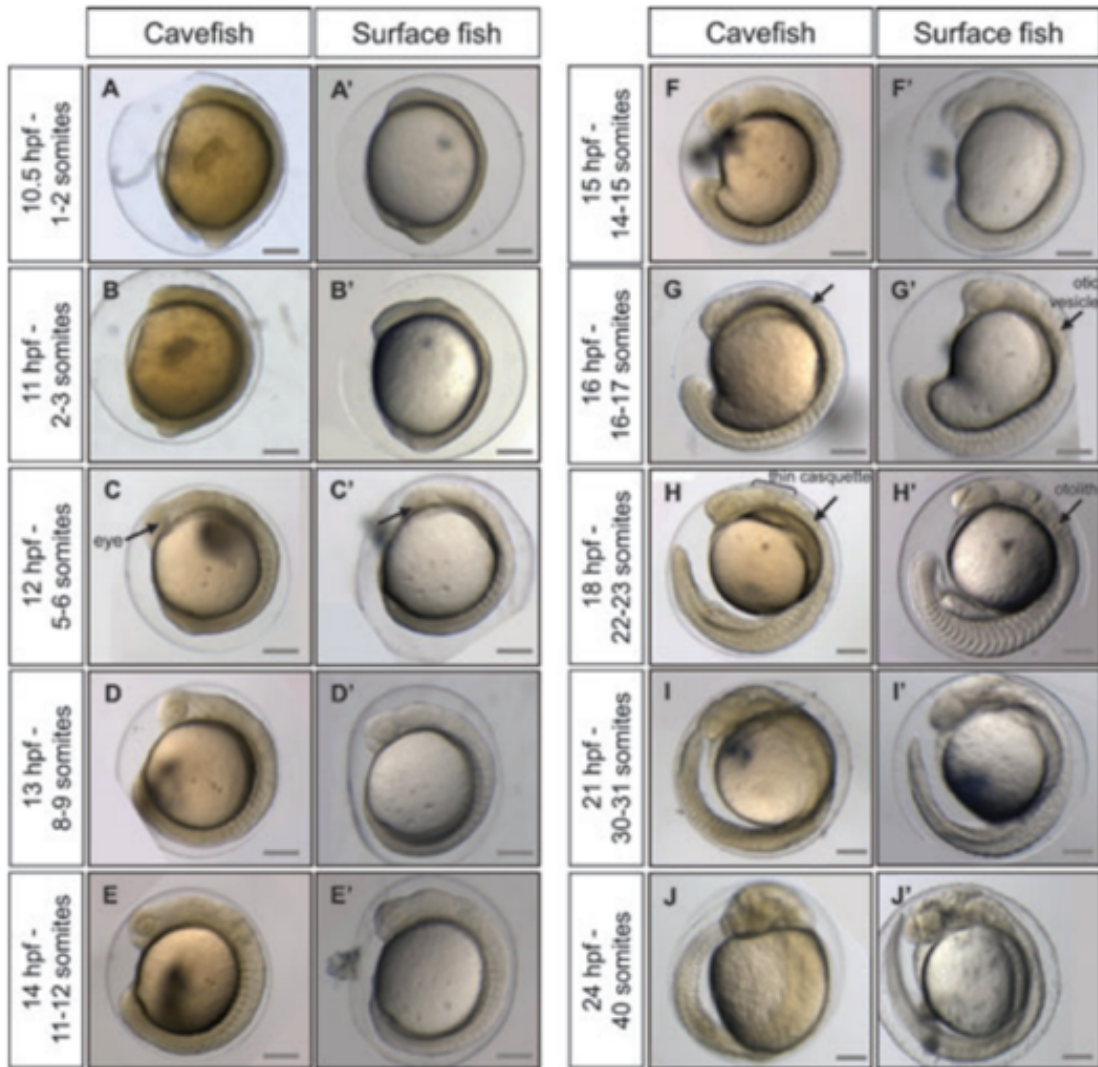
Figure 13: Images compare cave fish and surface fish larvae from 10.5 hours post fertilization to 24 hours post fertilization (Hinaux, 2011, p. 157).
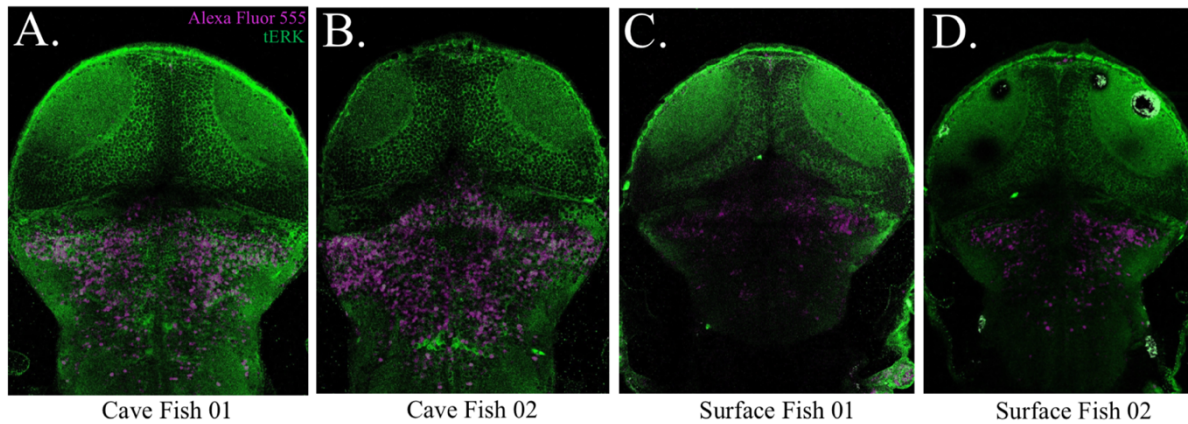
Results

2-Photon Microscopy

The third trial of the protocol was successful in that the 2-photon microscopy detected proliferative cells with EdU and they were regionalized using tERK. Purple cells on 2-photon images indicate EdU-positive cells while green structures resemble the entire brain of each morph (**Results Figure 1**). There are clear differences between the surface fish and cave fish,
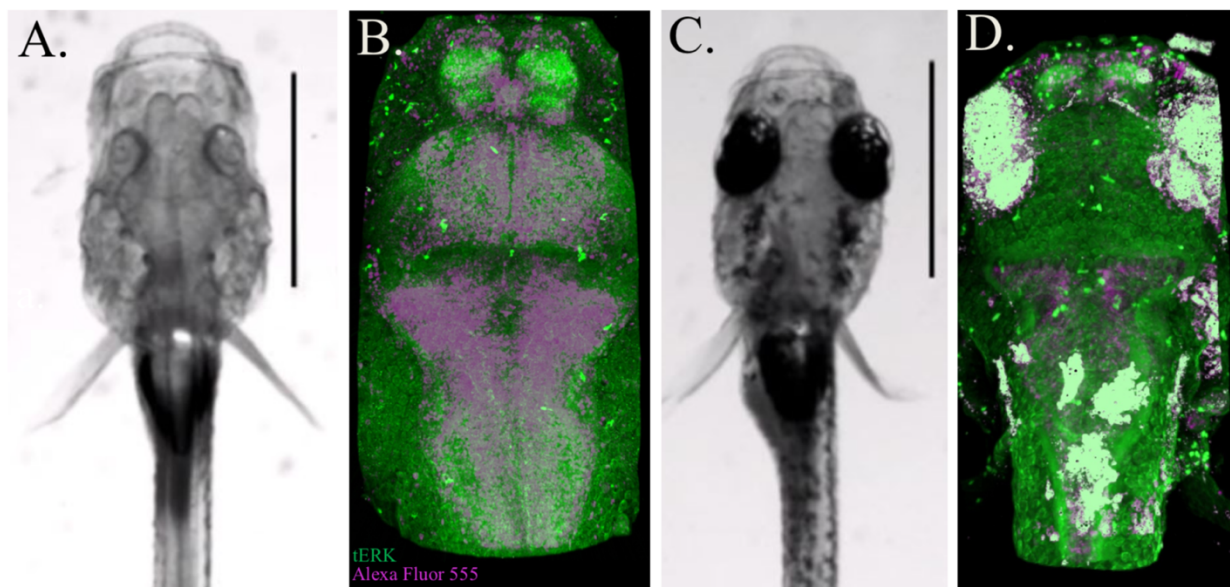
Results Figure 1: A dorsal view of cave fish and surface fish larvae respectively. A. is a larval cave fish, and B. is a 3D rendering of the tERK (in green) and Alexa Fluor-stained cells (in purple), imaged with a 2-photon microscope, in a cave fish that was incubated in EdU at 24 hours post fertilization and fixed at 6 days post fertilization. C. is a larval surface fish, and D. is a 3D rendering of tERK (in green) and Alexa fluor stained cells (in purple), from 2- photon microscope imaging, in a surface fish that was incubated in EdU at 24 hours post fertilization and fixed at 6 days post fertilization.

most evidently in the dorsal rhombencephalon that shows less ventral proliferation in the surface morph compared to the cave morph (**Results Figure 2**). Given that the preliminary results are the first successful rendition of the protocol, there were still some fixation issues encountered that affected hypothalamic visibility. Although, the ventral-most readable aspect of the stain appears

to concur with the hypothesis from face value. The optic tectum shows similar proliferation across morphs and quantification is necessary to make any conclusions (Figure 3 & 4 & 5).


Results Figure 2: The ventral region of the optic tectum and dorsal rhombencephalon, posterior to the optic tectum. The purple cells within the rhombencephalon are stained with Alexa Fluor dye and were proliferative at the time of EdU incubation (24 hours post fertilization). A. and B. are both cross-sections of the cave fish brain while C. and D. are from the surface fish. D. presents dark spots from interference with the laser caused by the surface fish pigment, particularly the eyes.
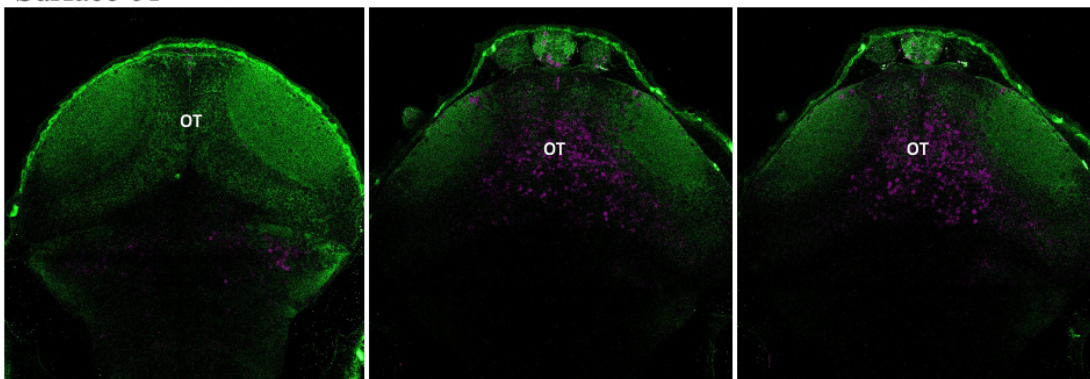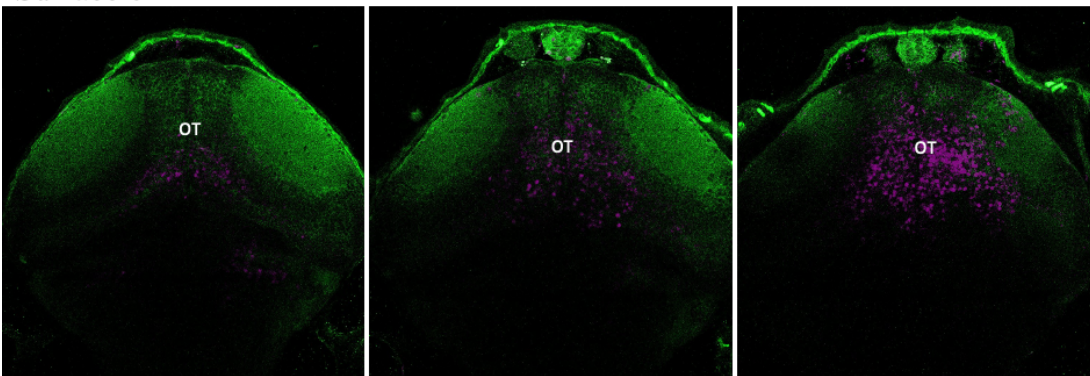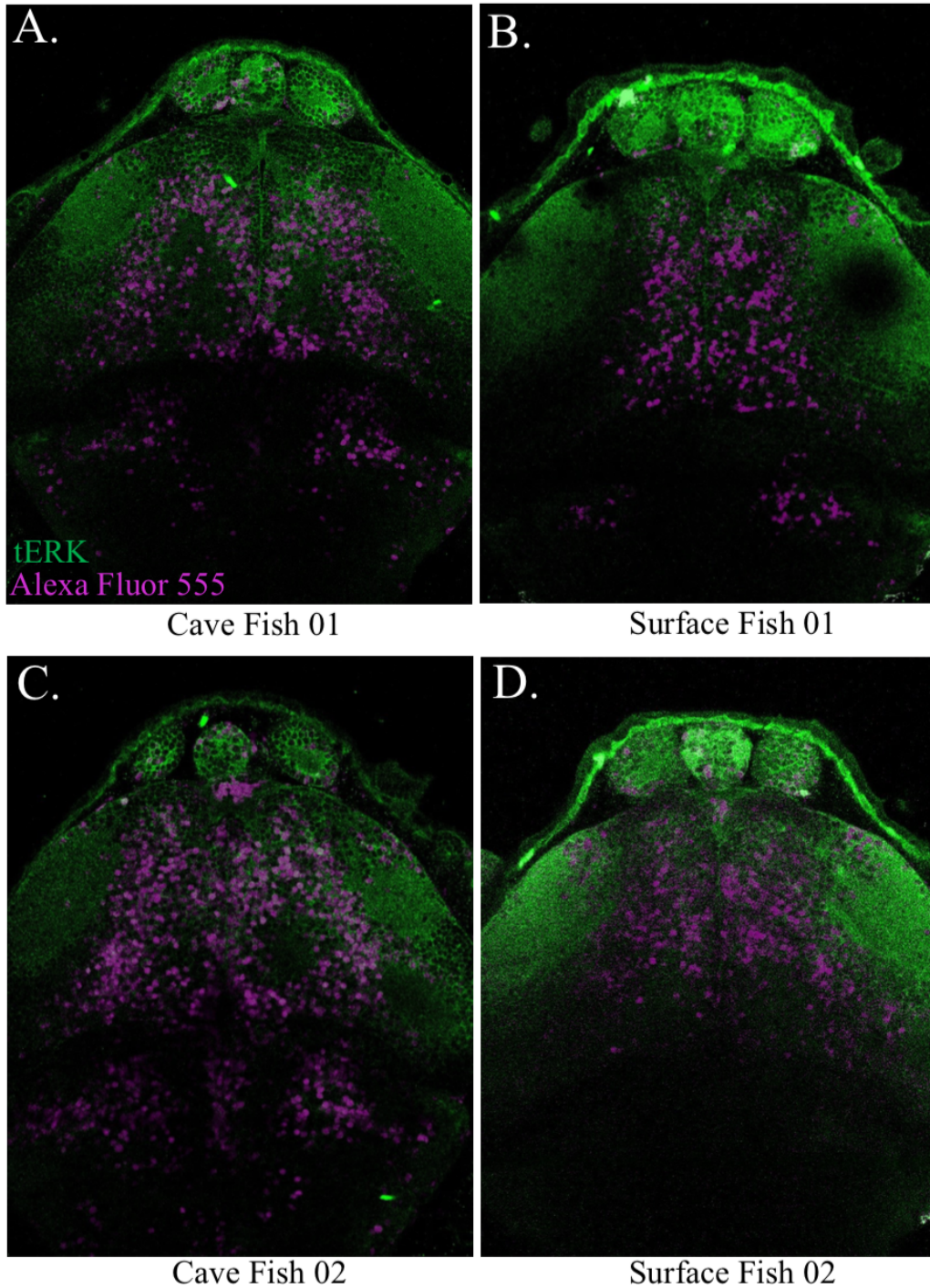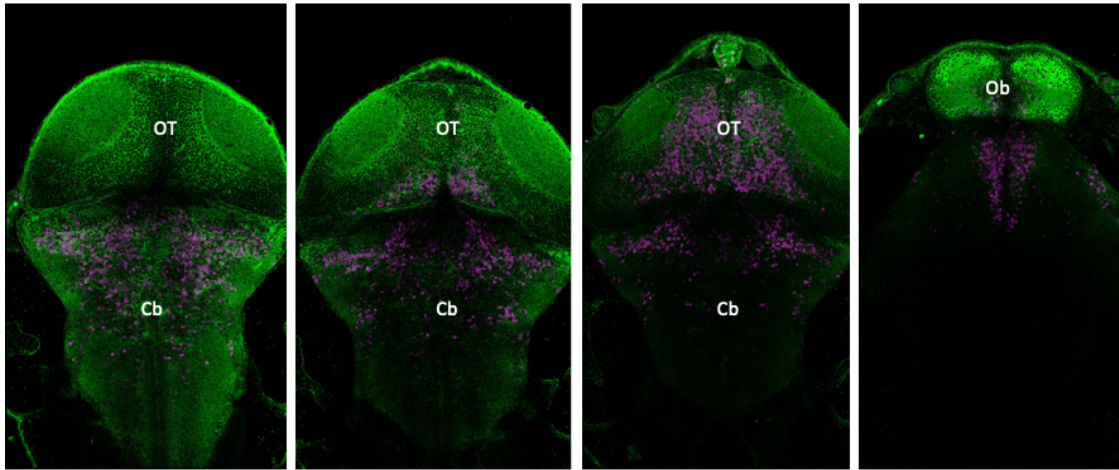

Results Figure 3: Slices of the Z-stack from 2-photon microscopy in two surface morph samples that highlight the optic tectum. As the images move from left to right, they are more dorsal, closer to the top of the sample. OT denotes the optic tectum.

Results Figure 4: Images that each reside at the same location within a Z-stack taken by the 2-photon microscope. The microscope has detected Alexa Fluor dye (purple) and tERK (green), with all images highlighting the optic tectum. A. and C. are from separate cave fish while B. and D. are from separate surface fish. The purple cells within the mesencephalon are stained with Alexa Fluor dye and were proliferative at the time of EdU incubation (24 hours post fertilization). The optic tectum, outlined by tERK, is the anterior structure comprised of two lobes.

Pachón 01

Pachón 02
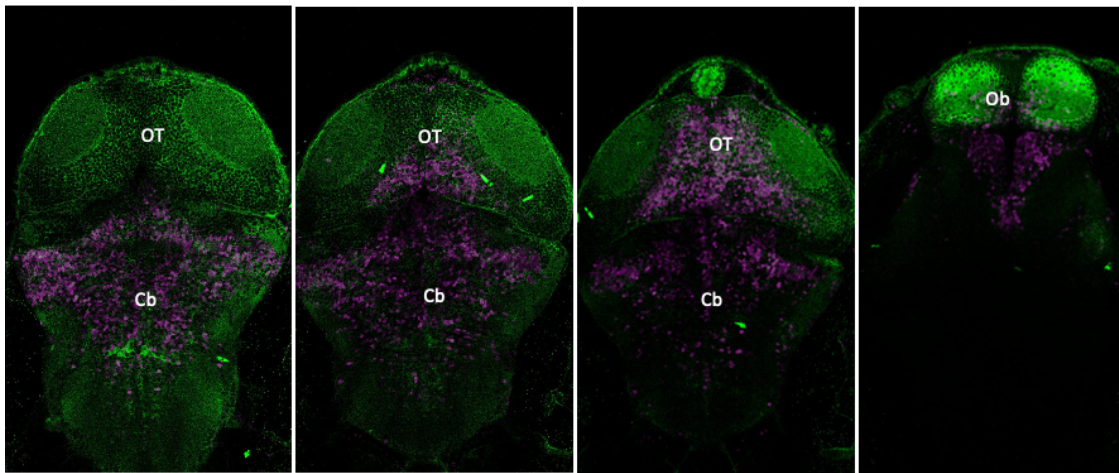
Results Figure 5: Slices of the Z-stack from 2-photon microscopy in Pachón samples. As the images move from left to right, they are more dorsal, closer to the top of the sample. OT denotes the optic tectum; Cb denotes the cerebellum; Ob denotes the olfactory bulbs.

Using manual segmentation in three dimensions on IMARIS software as demonstrated in Results Figure 6, we performed quantification of preliminary images. Optic tectum proliferation shows a higher percentage EdU-positive cells in surface fish (27.6% vs. 18.3%). Surface fish also recorded a higher overall volume of the optic tectum ($2.18 \times 10\text{-}7\mu m^3$ vs. $1.49 \times 10\text{-}7\mu m^3$) which shows consistency with previous studies (**Results Table 1, Results Figure 7 & 8**) (Kozol, 2022).
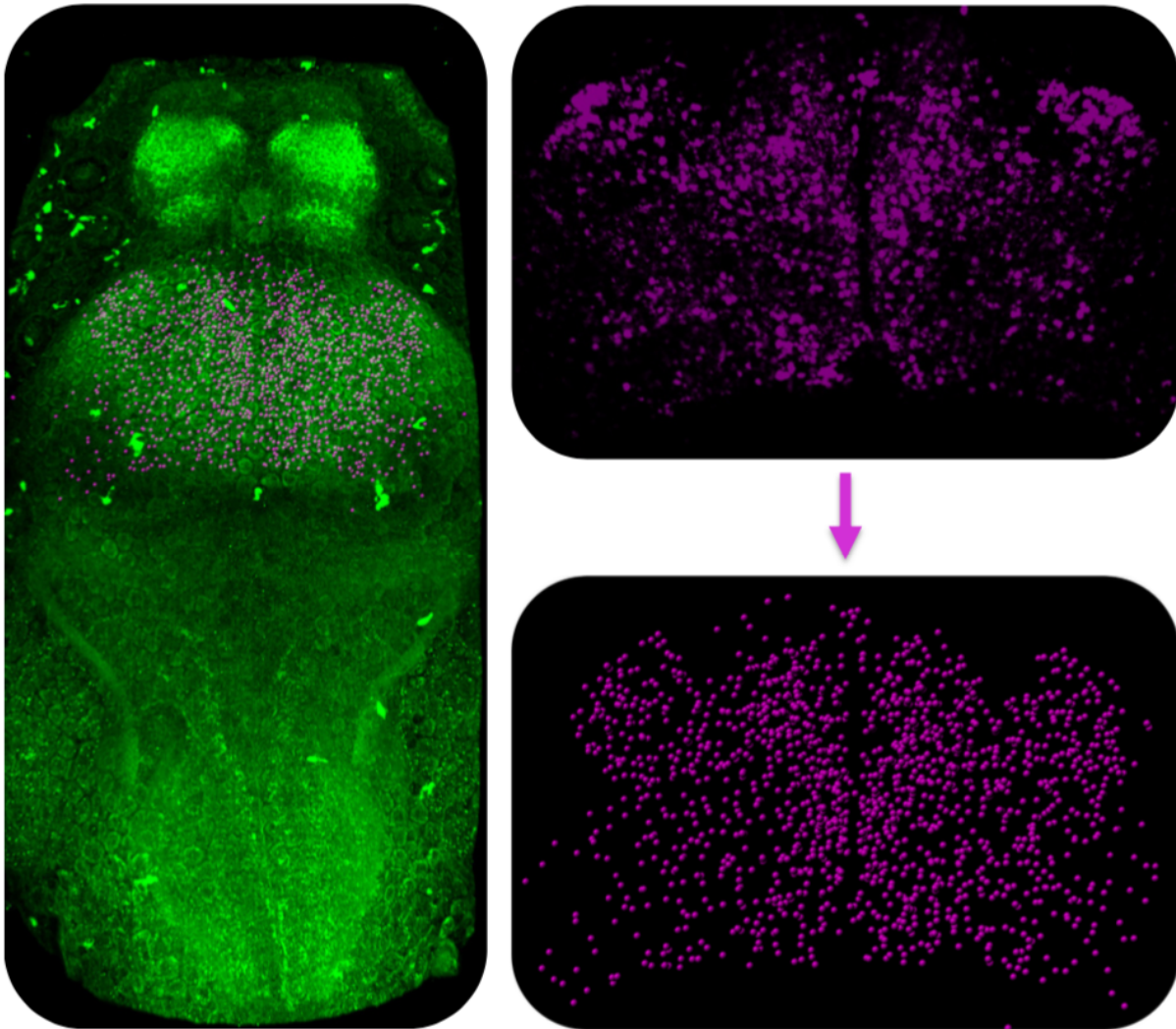
Results Figure 6: The technique by which cells were quantified. The Alexa-stained cells of the optic tectum were isolated by manual segmentation, and a 3D model of counted proliferative cells was rendered using IMARIS software.

Preliminary Quantification Results of the Optic Tectum

Sample	Noise	OT Cells	Total Cells	% Total	OT Volume (μm^3)	Cells /μm^3
PA 01		1533	7762	19.75	1.85E+07	8.28649E-05
PA 02		3119	18500	16.86	1.12E+07	2.78E-04
SF 01	1982	1291	4429	29.15	1.49E+07	8.66E-05
SF 03	809	1891	5327	35.50	2.27E+07	8.33E-05
SF 04	617	1498	8214	18.24	2.78E+07	5.39E-05

Results Table 1: The number of EdU positive cells, specifically within the optic tectum of the samples. PA denotes Pachón and SF denotes surface fish. Proliferative cells in the optic tectum were calculated as a percentage of total EdU positive cells to account for any discrepancies in staining. Noise denotes the number of cells counted by IMARIS software, that are false positives, due to interference of the eye pigment in surface fish with the 2-photon laser in that portion of the scan.
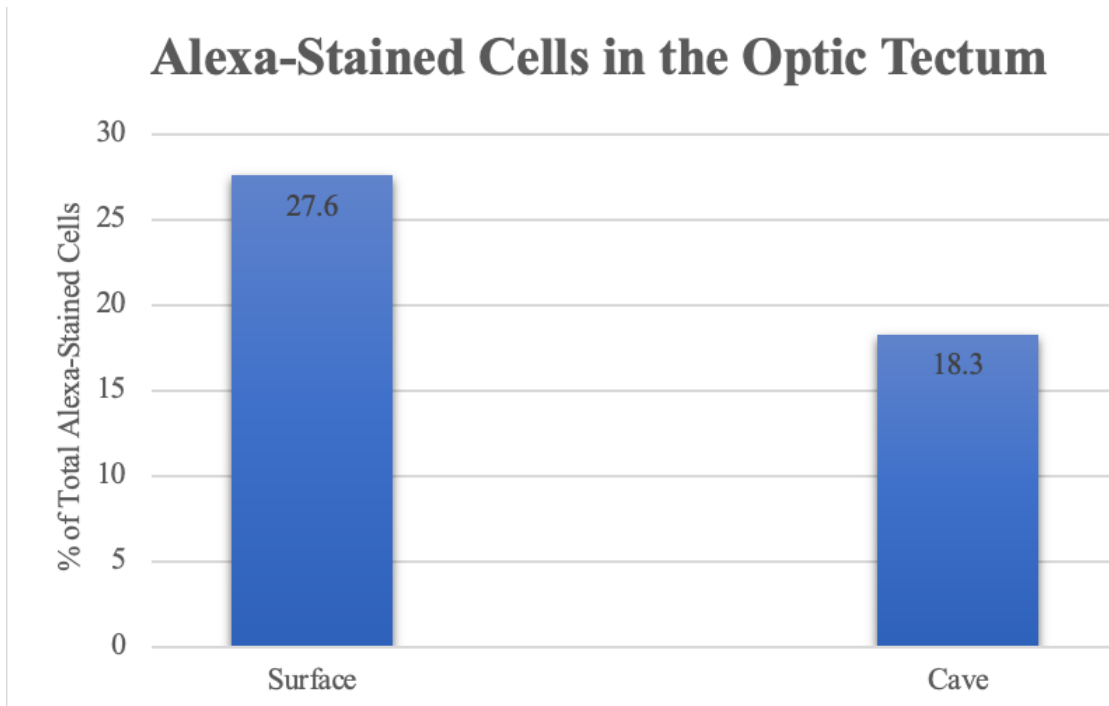
Results Figure 7: Comparison of EdU positive (and Alexa-stained) cells found in the optic tectum of surface and cave morphs as the percentage of total EdU positive cells in the sample.
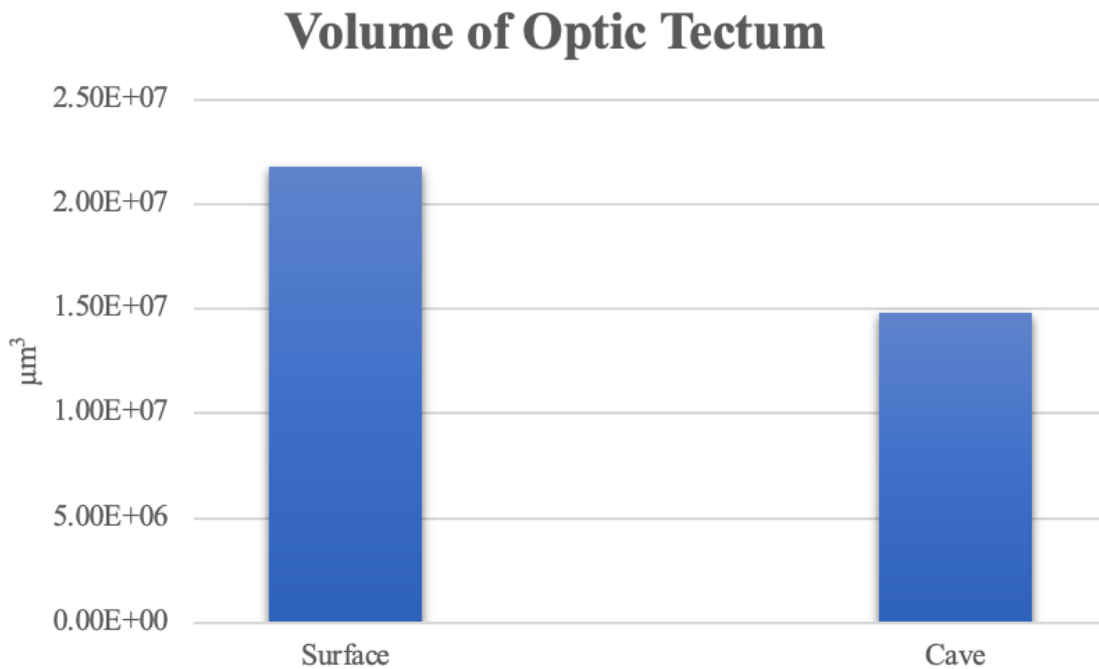
Results Figure 8: The average volume of the manually segmented optic tectum region, measured in μm^3, across cave and surface morphs.

Discussion

By conducting a series of experiments using EdU immunostaining, we aimed to discover what biological mechanisms regulate the differentiation of neuroanatomical traits. An effective EdU immunostaining protocol was utilized to detect proliferative cells across *Astyanax mexicanus* morphs. As the 2-photon images demonstrated, immunohistochemistry using t-ERK was also successful in mapping the total brain area. By altering a technique typically used for isolated cell culture, the protocol gave us the ability to stain cells within the live *Astyanax* for the very first time! Staining showed the final location of proliferative cells in larvae six days old, and preliminary counting of Alexa-positive cells revealed a higher percentage of cells present in the optic tectum of the surface fish compared to the cave fish. Although, the staining lacked strong penetrance in the most ventral regions of the samples, specifically the hypothalamus, making proliferation comparisons inconclusive. Yet, upon initial inspection of the most ventral-caudal regions (**Results Figure 2**), the variation in neurogenesis across morphologies, as seen evidently in the cerebellum, could be indicative of an increase associated with re-directed retinal cells in the cave morph. Although, given that the sample size was only five for preliminary data analysis, in order to identify significant trends, cell counting should be executed on many more fish, that are prepped and ready to be imaged by the Duboué lab.

Future additions to the protocol would involve lineage tracing to demonstrate the exact location on the embryo from which the proliferative cells in the hypothalamus and optic tectum (at 6 dpf) originated. After gathering further support for the patterned redirection of retinal cells in the cave morph, the laboratory could aim to identify a developmental gene that regulates the distribution of proliferative cells in both the optic tectum and the hypothalamus that could be causal to the reciprocal relationship of their volumes. Identifying a genetic mutation contributing

to altered distribution of proliferative cells in cave fish and surface fish could allow for further understanding of how neuroanatomic traits develop and diverge to best suit an organism to their environment. Given the genetic and neuronal similarities between fish and high order mammals, EdU immunostaining will elucidate mechanisms of evolution that can in turn be used to inform predictive models of how the brain adapts to the human condition. With a rapidly changing climate and an increasingly interconnected, digital world, there are many new problems that people must face on a daily basis. As humanity must confront more pressures in a highly globalized environment that did not exist twenty years ago, it would be very useful to understand how they may be forcing the human brain to adapt, along with potential repercussions or benefits.

Acknowledgements

References

Buck, S., Bradford, J., Gee, K., Agnew, B., Clarke, S., & Salic, A. (n.d.). Detection of S-phase cell cycle progression using 5-ethynyl-2'-deoxyuridine incorporation with click chemistry, an alternative to using 5-bromo-2'-deoxyuridine antibodies. *BioTechniques*, *44*(7), 927-929. https://doi.org/10.2144/000112812

Click-IT® Edu Imaging Kits Protocol. Thermo Fisher Scientific - US. (n.d.). Retrieved October 26, 2022, from https://www.thermofisher.com/us/en/home/references/protocols/cell-and-tissue-analysis/protocols/click-it-edu-imaging-protocol.html

Hinaux, H., Pottin, K., Chalhoub, H., Père, S., Elipot, Y., Legendre, L., & Rétaux, S. (2011). A developmental staging table for Astyanax mexicanus surface fish and Pachón cave fish. *Zebrafish*, *8*(4), 155–165. https://doi.org/10.1089/zeb.2011.0713

Jeffery, W. R. (2020). Astyanax surface and cave fish morphs. *EvoDevo*, *11, 14 (2020)*. https://doi.org/10.1186/s13227-020-00159-6

Jeffery, W. R. (2009). Evolution and development in the cave fish Astyanax. *Current Topics in Developmental Biology*, *86*, 191–221. https://doi.org/10.1016/S0070-2153(09)01008-4

Kawakami, K., & Murakami, Y. (2017). *Diversity of Vertebrate Brains*. Wiley Online Library. John Wiley and Sons, Inc. Retrieved from https://onlinelibrary.wiley.com/doi/full/10.1111/dgd.12375#:~:text=For%20example%2C%20the%20brains%20of,the%20basic%20structures%20during%20evolution.

Kawakami, K. and Murakami, Y. (2017), Preface to Vertebrate Brains: evolution, structures, and functions. Develop. Growth Differ., 59: 160-162. https://doi.org/10.1111/dgd.12375

Kimmel, C. B., Ballard, W. W., Kimmel, S. R., Ullmann, B., & Schilling, T. F. (1995, July). *Stages of Embryonic Development of the Zebrafish* . American Association for Anatomy. Retrieved October 25, 2022, from https://anatomypubs.onlinelibrary.wiley.com/doi/10.1002/aja.1002030302

Kozol, R. A., Conith, A. J., Yuiska, A., Cree-Newman, A., Tolentino, B., Banesh, K., Paz, A., Lloyd, E., Kowalko, J. E., Keene, A. C., Albertson, R. C., & Duboue, E. R. (2022). A brain-wide analysis maps structural evolution to distinct anatomical modules. *BioRxiv*, 2022.03.17.484801. https://doi.org/10.1101/2022.03.17.484801
Pottin et al 2011

Ma, L., Dessiatoun, R., Shi, J., & Jeffery, W. R. (2021). Incremental Temperature Changes for Maximal Breeding and Spawning in Astyanax mexicanus. *Journal of visualized experiments : JoVE*, (168), 10.3791/61708. https://doi.org/10.3791/61708

Northcutt, R. G. (2002). Understanding Vertebrate Brain Evolution. *Integrative and Comparative Biology*, *42*(4), 743–756. http://www.jstor.org/stable/3885002

Nwe, K., & Brechbiel, M. W. (2009). Growing applications of "click chemistry" for bioconjugation in contemporary biomedical research. *Cancer biotherapy & radiopharmaceuticals*, *24*(3), 289–302. https://doi.org/10.1089/cbr.2008.0626

Rétaux, S., Alié, A., Blin, M., Devos, L., Elipot, Y., & Hinaux, H. (2016). *Neural Development and Evolution in Astyanax mexicanus: Comparing Cave fish and Surface Fish Brains* (pp. 227–244). https://doi.org/10.1016/B978-0-12-802148-4.00012-8

y Cajal, S. R. (1999). Neural Centers. In *Texture of the Nervous System of Man and the Vertebrates: Volume I An annotated and edited translation of the original Spanish text with the additions of the French version by Pedro Pasik and Tauba Pasik* (pp. 249–262). Springer Vienna. https://doi.org/10.1007/978-3-7091-6435-8_10

Zhang, G. (2021). *Vertebrate Evolution* . SciTechDaily. University of Copenhagen . Retrieved from https://scitechdaily.com/surprise-were-more-like-primitive-fishes-than-once-believed/amp/.